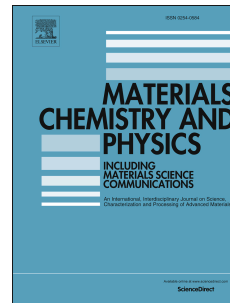# Accepted Manuscript

Capacitive performance of cysteamine functionalized carbon nanotubes

Gomaa A.M. Ali, Ellie Yi Lih Teo, Eslam A.A. Aboelazm, Hamidreza Sadegh, Amir O.H. Memar, Ramin Shahryari-Ghoshekandi, Kwok Feng Chong

Please cite this article as: G.A.M. Ali, E.Y. Lih Teo, E.A.A. Aboelazm, H. Sadegh, A.O.H. Memar, R. Shahryari-Ghoshekandi, K.F. Chong, Capacitive performance of cysteamine functionalized carbon nanotubes, *Materials Chemistry and Physics* (2017), doi: 10.1016/j.matchemphys.2017.05.019.

Capacitive Performance of Cysteamine Functionalized Carbon Nanotubes

Gomaa A. M. Ali [a,b], Ellie Yi Lih Teo [a], Eslam A. A. Aboelazm [a], Hamidreza Sadegh [c,*],

Amir O. H. Memar [d], Ramin Shahryari-Ghoshekandi [c], Kwok Feng Chong [a,**]

[a] Faculty of Industrial Sciences & Technology, Universiti Malaysia Pahang, Gambang, 26300 Kuantan, Malaysia

[b] Chemistry Department, Faculty of Science, Al–Azhar University, Assiut, 71524, Egypt

[c] Department of Chemistry, Science and Research Branch, Islamic Azad University, Tehran, Iran

[d] Young Researchers and Elite Club, Science and Research Branch, Islamic Azad University, Tehran, Iran

[*] Corresponding author: Email: h.sadegh@chemist.com, hamidreza.sadegh@srbiau.ac.ir

[**] Corresponding author: Email: ckfeng@ump.edu.my (Tel.: +609 5492403; Fax: +609 5492766)

Abstract

We report on the capacitive performance of redox active cysteamine-functionalized multi walled carbon nanotubes (MWCNTs-Cyst). The thiol functional groups are found to be oxidized into sulfinic acid groups during functionalization of MWCNTs-Cyst, rendering the functional groups act as the molecular spacer to prevent MWCNTs agglomeration and the redox active sulfinic acid groups provides pseudocapacitance effect. The specific capacitance attained on MWCNTs-Cyst is found to be approximately 4-times higher than the nonfunctionalized MWCNTs electrodes. The enhancement can be attributed to the surface area enhancement in MWCNTs-Cyst and the pseudocapacitance effect. *Ex situ* spectroscopy (XPS and FTIR) confirms pseudocapacitive behavior of sulfinic acid groups, which undergo redox reaction into sulfenic acid groups upon charging and discharging process. Impedance study reveals the charge transfer process is facilitated by the redox reaction of sulfinic acid groups, thus lowering the charge transfer resistance. Interestingly, the supercapacitor made from MWCNTs-Cyst remains highly stable (90% retention) even after long cycle of charge discharge operation (11000 cycles).

Keywords: Carbon; Charge storage; Supercapacitors; Double layer capacitance; Redox.

1. Introduction

With the growing world population and increasing standard of living, global demand for energy is increasing substantially. The energy storage system is, therefore crucial in supplying huge amount of energy whenever it is needed. In this context, supercapacitors emerge as the promising energy storage device as they could deliver high energy density ($\geq$ 5 Wh kg^{-1}) at fast rate ($\geq$ 10 kW kg^{-1}) [1]. Credit to nanotechnology, supercapacitors technology advances remarkably by utilizing nanostructured electrodes, which possess exceptionally high surface area and other superior physicochemical properties. Carbon nanotubes (CNTs) is one of the nanomaterials emerges from this technology revolution and used in supercapacitors electrode.

CNTs is a cylindrical carbon nanostructure that discovered in 1991 by Iijima in the carbon soot made by arc-discharge method [2]. Due to its unique structure, CNTs possesses extraordinary properties, such as high theoretical specific surface area (range from 50 to 1315 m^2 g^{-1}), high length-to-diameter ratio (132,000,000 to 1), outstanding thermal conductivity and electrical properties [3-6]. Hence, CNTs receives intense research attention worldwide in various applications, from biomedical, to energy system and to environmental remediation [7-17]. The application of CNTs in supercapacitors was pioneered by Niu et al., who produced high-power supercapacitors with free-standing mats of CNTs [18]. The work is remarkable as it shows the open structure of CNTs enables entire surface area for the ions adsorption, unlike activated carbon that only utilizes 1/3 of the surface area for this purpose. Other report by Frackowiak et al. suggested that the presence of mesopores formed by the entanglement of carbon nanotubes also contributes to the improved ions adsorption [19] . To date, numerous works have been reported on the fabrication of supercapacitors electrode by CNTs, mostly in the form of multiwalled carbon nanotubes (MWCNTs) due to its ease of scale-up production. The quality of MWCNTs however is often being compromised during scale-up production, leading to poor performance of MWCNTs. Strong acid treatment for the oxidation of MWCNTs surface is often used to improve MWCNTs' performance by introducing oxygen functional groups for the pseudocapacitance effect [20]. For oxygen functionalized MWCNTs, 2-fold capacitance enhancement was achieved, however, at the expense of cycling stability [21]. Therefore, it is of great importance to engineer the MWCNTs surface for capacitance enhancement while preserving its cycling stability. In this work, industrial-grade MWCNTs is functionalized with cysteamine group for the capacitive enhancement and its redox reaction is investigated by e*x situ* spectroscopy techniques.

2

2. Experimental method

Multi-walled carbon nanotubes (MWCNTs) (purity >95%; outer diameter 40–60 nm; length 5–20 μm) made from catalytic chemical vapor deposition were purchased from US Research Nanomaterials, Inc. Sulfuric acid (H_2SO_4: 97%, AR grade), nitric acid (HNO_3: 37%, AR grade), hydrochloric acid (HCl: 37%, AR grade) and cysteamine hydrochloride ($HSCH_2CH_2NH_2 \cdot HCl$: 99%) were purchased from Sigma-Aldrich. 1-ethyl-(3-3′-dimethylaminopropyl) carbodiimide ($C_8H_{17}N_3$: EDC: 97%) and N-hydroxysuccinimide ($C_4H_5NO_3$: NHS: 99%) were purchased from Merck Millipore. All the chemicals were used as received unless otherwise stated. The MWCNTs treatment and functionalization were performed as our previous report [22]. Briefly, pure MWCNTs (1 g) was purified in 20% HCl for 120 min, followed by reflux oxidation in a mixture of concentrated HNO_3 and H_2SO_4 (1:3, v/v) at 75 °C for 6 h. The oxidized MWCNTs was filtered, washed thoroughly by deionized water and dried in vacuum at 80 °C for 120 min. The cysteamine functionalization of MWCNTs was done by carbodiimide chemistry to link the amine group of cysteamine and the COOH of oxidized MWCNTs. Oxidized MWCNTs (100 mg) was added into the ethanolic solution (25 mL) containing cysteamine HCl (30 mg), EDC (35 mg) and NHS (20 mg), followed by refluxing at 50 °C for 48 h. The cysteamine functionalized MWCNTs (MWCNTs-Cyst) was collected after filtration, washing and vacuum drying. The oxidation state of sulfur in MWCNTs was studied by X-ray photoelectron spectrometer (XPS; Ulvac-Phi/Phi 5000 Versaprobe II spectrometer). The surface morphology was studied by field emission scanning electron microscope (FESEM; JEOL 1525) and the surface area was investigated by surface area analyzer (NOVA 3200). Thermogravimetric analysis (TGA) was performed under nitrogen atmosphere at a heating rate of 5 °C min^{-1} using thermogravimetric analyzer (Mettler Toledo TGA DSC 1).

Electrochemical studies were performed in two-electrode system, by an AUTOLAB PGSTAT101 potentiostat/galvanostat with frequency response analyzer. The electrodes were prepared from the active materials, carbon black and polyvinylidene fluoride in the weight ratio of 90:5:5. A porous membrane pre-soaked with 1 M Na_2SO_4 electrolyte was used as the separator. Electrochemical impedance spectroscopy (EIS) data were collected from 500 kHz to 0.01 Hz, at open circuit potential (OCP) with a.c. amplitude of 10 mV. The electrode changes during charge discharge process was investigated *ex situ* by Fourier transform infrared spectrometer (FTIR; Perkin Elmer Spectrum 100) and XPS spectrometer.

3. Results and discussion

Fig. 1a shows the FESEM image of MWCNTs-Cyst. The cysteamine functionalization does not alter the morphology of MWCNTs and they remain as tubular shape with entanglement. Such open space morphology is crucial for the charge adsorption in energy storage process. The presence of sulfur in MWCNTs-Cyst is substantiated by the sulfur elemental map shown in Fig. S1. EDX analysis reveals the sulfur content of 2.5% and they are evenly distributed in MWCNTs-Cyst. As thiol is the main functional groups in the MWCNT-Cyst, the sulfur oxidation states were investigated by XPS analysis and its results for S 2p is depicted in Fig. 1b. It should be noted that each deconvoluted S 2p component should have S $2p_{3/2}$ and S $2p_{1/2}$ doublet with an intensity ratio of 2:1, and with an energy separation of 1.2 eV [23, 24]. There are two broad peaks can be observed for the S 2p analysis of MWCNTs-Cyst. The first peak can be deconvoluted into binding energy of 162.9 eV (S $2p_{3/2}$) and 164.1 eV (S $2p_{1/2}$), which is attributed to the thiol groups (SH); The second peak can be deconvoluted into binding energy of 170.0 eV (S $2p_{3/2}$) and 171.2 eV (S $2p_{1/2}$), which can be attributed to the sulfinic acid (SOOH) groups. The findings suggest that part of the thiol groups in cysteamine has been oxidized into sulfinic acid group (SOOH) during the functionalization process of MWCNTs-Cyst. The degree of thiol functionalization was evaluated by thermal analysis, as shown in Fig. 1c. The MWCNTs has minimal weight loss up to 500 °C and the weight loss beyond this point could be attributed to the decomposition of MWCNTs. On the other hand, MWCNTs-Cyst has comparatively better thermal stability up to 500 °C, which could be associated to the lower adsorbed water due to the cysteamine groups. Nonetheless, MWCNTs-Cyst suffers substantial weight loss at temperature higher than 500 °C as the decomposition of MWCNTs occurs simultaneously with the decomposition of cysteamine groups. The specific surface area for MWCNTs and MWCNTs-Cyst were calculated by Brunauer–Emmett–Teller (BET) theory (Fig. 1d). Due to the mass production of industrial grade MWCNTs, the quality of MWCNTs could be compromised, thus producing low specific surface area of 26.3 m^2 g^{-1} of as-received MWCNTs. Upon cysteamine functionalization, it creates repulsion force which prevents the tubes agglomeration and appreciably increases the specific surface area of MWCNTs-Cyst up to 94.9 m^2 g^{-1}. Such increment in surface area is crucial for the ions adsorption for energy storage.

Fig. 2a shows the cyclic voltammograms (CV) of MWCNTs and MWCNTs-Cyst in 1 M Na_2SO_4 electrolyte with 2-electrode system. The symmetric 2 electrodes are charged and

discharged at a pseudoconstant rate over the entire voltammetric cycles, resulting in the absence of redox peaks in CV [25]. The area under the curve represents the total charge accumulation and it shows that the MWCNTs-Cyst electrode has higher charge accumulation as compared to the MWCNTs electrode. The charge discharge (CDC) curve of MWCNTs-Cyst is highly symmetrical, indicating the reversibility of charge storage in MWCNTs-Cyst. In addition, its linear CDC curves signifies the rapid current-voltage response in MWCNTs-Cyst. The specific capacitance of MWCNTs-Cyst and MWCNTs were calculated from the slope of discharge curve using equation reported elsewhere [1, 26] and they are summarized in Fig. 2c. As suggested by CV analyses, MWCNTs-Cyst shows higher charge storage ability by having higher specific capacitance as compared to that of MWCNTs. The highest specific capacitance of 23 F g^{-1} is attained by MWCNTs-Cyst at 0.25 A g^{-1}, which is 4-fold increment as compared to that of MWCNTs (6 F g^{-1}). This is in consistence with the 4-fold increment in the specific surface area from 26.3 to 94.9 m^2 g^{-1} as discussed above. The specific capacitance enhancement for MWCNTs-Cyst could be attributed to the cysteamine functionalization, which acts as the molecular spacer to avoid tubes agglomeration, therefore producing larger surface area for the ions adsorption. Besides, the sulfinic acid functional groups in MWCNTs-Cyst could possibly possess redox activity which enhances specific capacitance by pseudocapacitance effect. Therefore, *ex situ* spectroscopies (XPS and FTIR) were employed to study the chemical changes in cysteamine group during charge storage process. It can be observed from the XPS analyses (Fig. 2d) that the all the sulfur peaks are shifted to higher binding energy for MWCNTs-Cyst after charging process. It suggests the charging process oxidizes both thiol and sulfinic acid groups in MWCNTs-Cyst. Upon discharging process (Fig. 2e), all the sulfur peaks are shifted to lower binding energy (168.4 eV and 169.6 eV), which can be ascribed to the sulfenic acid groups (SOH). The XPS findings are supported by the FTIR analysis (Fig. 2f). The sulfenic acid in charged MWCNTs-Cyst could be observed in infrared absorption bands at 3461, 1102 and 645 cm^{-1}, corresponding to O-H, S=O and S-O stretching modes respectively. Similar infrared absorption bands are observed for discharged MWCNTs-Cyst, except for the diminishment of S=O stretching band which suggests the reduction into sulfenic acid groups. Based on the XPS and FTIR analyses, the redox reaction of MWCNTs-Cyst during CDC process is proposed as follows:
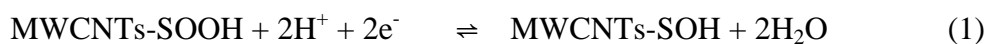
$$MWCNTs\text{-}SOOH + 2H^+ + 2e^- \underset{Discharge}{\overset{Charge}{\rightleftharpoons}} MWCNTs\text{-}SOH + 2H_2O \qquad (1)$$

Fig. 3a shows Nyquist plot for MWCNTs–Cyst at open circuit potential (OCP). The Nyquist plot shows a small semi–circle at the high frequency region, corresponding to the equivalent series resistance (ESR) and charge transfer resistance (R_{CT}). Both ESR and R_{CT} for MWCNTs-Cyst are estimated to be 0.81 and 0.18 Ω, respectively. The relatively low R_{CT} value as compared to the reported value for pristine MWCNTs (5.13 Ω) [27] indicates the charge transfer process in MWCNTs-Cyst is facilitated by the redox activity of sulfinic acid functional groups. A near-vertical line at low frequency is in accordance with the Warburg diffusion for capacitive behavior. The phase angle at low frequency is found to be 84° (Fig. 3a inset), which is very close to the ideal supercapacitor (90°) [27, 28]. The cycling stability of MWCNTs-Cyst was tested for 11000 CDC cycles at 0.25 A g^{-1} (Fig. 3b). There is slight capacitance loss after 5000 CDC cycles, probably due to the minor loss of reversible redox reactions. It is noteworthy that the MWCNTs-Cyst could retain high cycling stability of 90% for 11000 cycles, in spite of having active redox sulfinic acid groups. Furthermore, the CDC curves shape are retained at the end of the test cycle (Fig. 3b inset). It shows that the redox activity of sulfinic acid groups in MWCNTs-Cyst are highly reversible, which is in contrary to other reported redox groups which show deterioration over long cycle of CDC [29]. Thus, MWCNTs-Cyst could be a potential electrode material for high stability supercapacitor device.

4. Conclusions

The capacitive performance of MWCNTs is enhanced by cysteamine functionalization, producing highly reversible redox active MWCNTs-Cyst. XPS analysis reveals the oxidation of thiol groups into sulfinic acid groups during functionalization of MWCNTs-Cyst. BET analysis suggests the surface area increment in MWCNTs-Cyst, which provides higher ions adsorption for double layer capacitance. *Ex situ* XPS and FTIR analyses propose the redox transition of sulfinic acid and sulfenic acid in MWCNTs-Cyst during the charge-discharge process. The stable double layer capacitance and high reversibility of sulfinic/sulfenic acid during charge discharge process renders the MWCNTs-Cyst to retain 90% of its capacitance, even after 11000 CDC cycles. The findings suggest the MWCNTs-Cyst could be the electrode material for highly stable supercapacitors device.
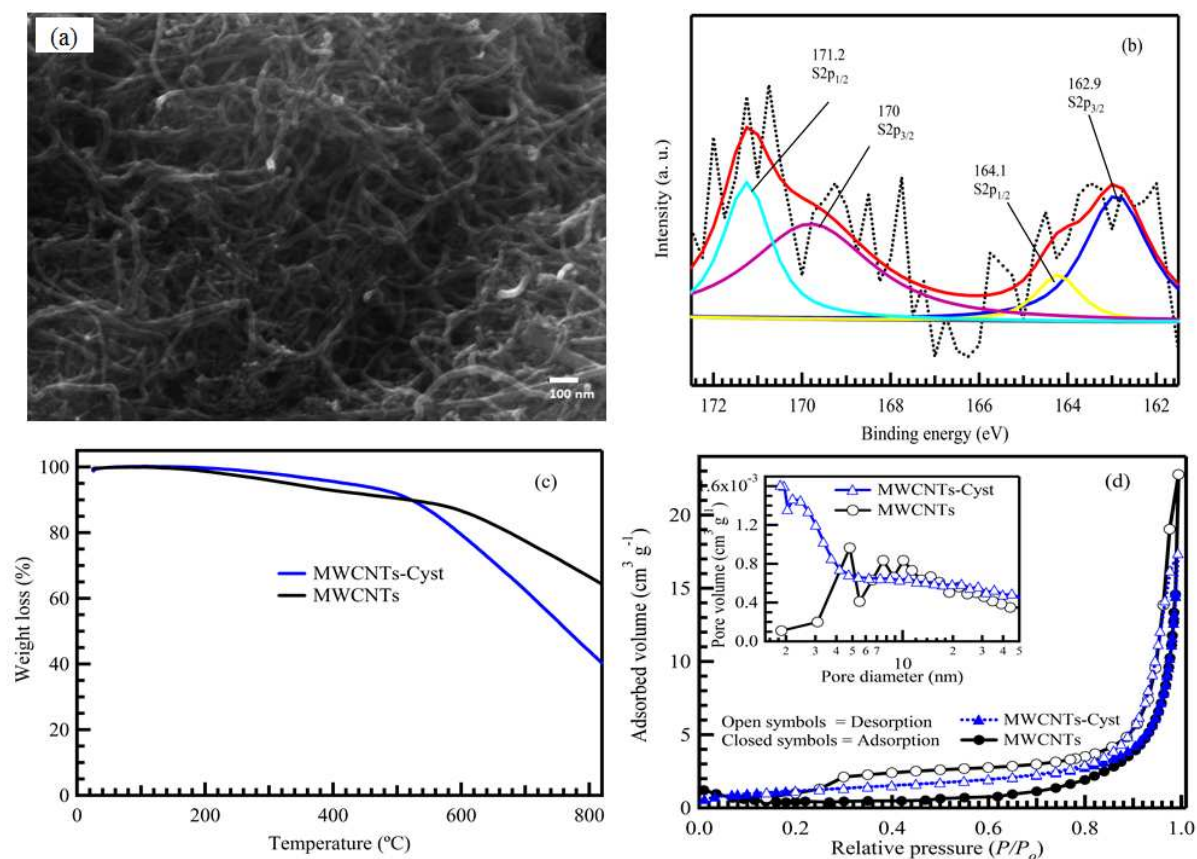
Acknowledgments

Figure Captions

Fig. 1. (a) FESEM image of MWCNTs-Cyst; (b) XPS S 2p spectrum of MWCNTs-Cyst; (c) TGA of MWCNTs and MWCNTs-Cyst; (d) Nitrogen adsorption-desorption curves for MWCNTs and MWCNTs-Cyst.

Fig. 2. (a) CV of MWCNTs and MWCNTs-Cyst at 25 mV s^{-1}; (b) CDC of MWCNTs and MWCNTs-Cyst at 0.25 A g^{-1} in 1 M Na_2SO_4 electrolyte; (c) Specific capacitance as a function of discharge current density; (d) XPS S 2p spectra of MWCNTs-Cyst after charged; (e) XPS S 2p spectra of MWCNTs-Cyst after discharged; (f) FTIR of MWCNTs-Cyst after charged and discharged.

Fig. 3. (a) EIS spectrum for MWCNTs-Cyst (Inset shows the Bode plot for phase angle); (b) Stability test for MWCNTs-Cyst for 11000 cycles (Insets show the CDC of 1st cycle and 11000th cycle).

Fig. 1. (a) FESEM image of MWCNTs-Cyst; Inset shows corresponding EDX sulfur mapping; (b) XPS S 2p spectrum of MWCNTs-Cyst; (c) TGA of MWCNTs and MWCNTs-Cyst; (d) Nitrogen adsorption-desorption curves for MWCNTs and MWCNTs-Cyst.
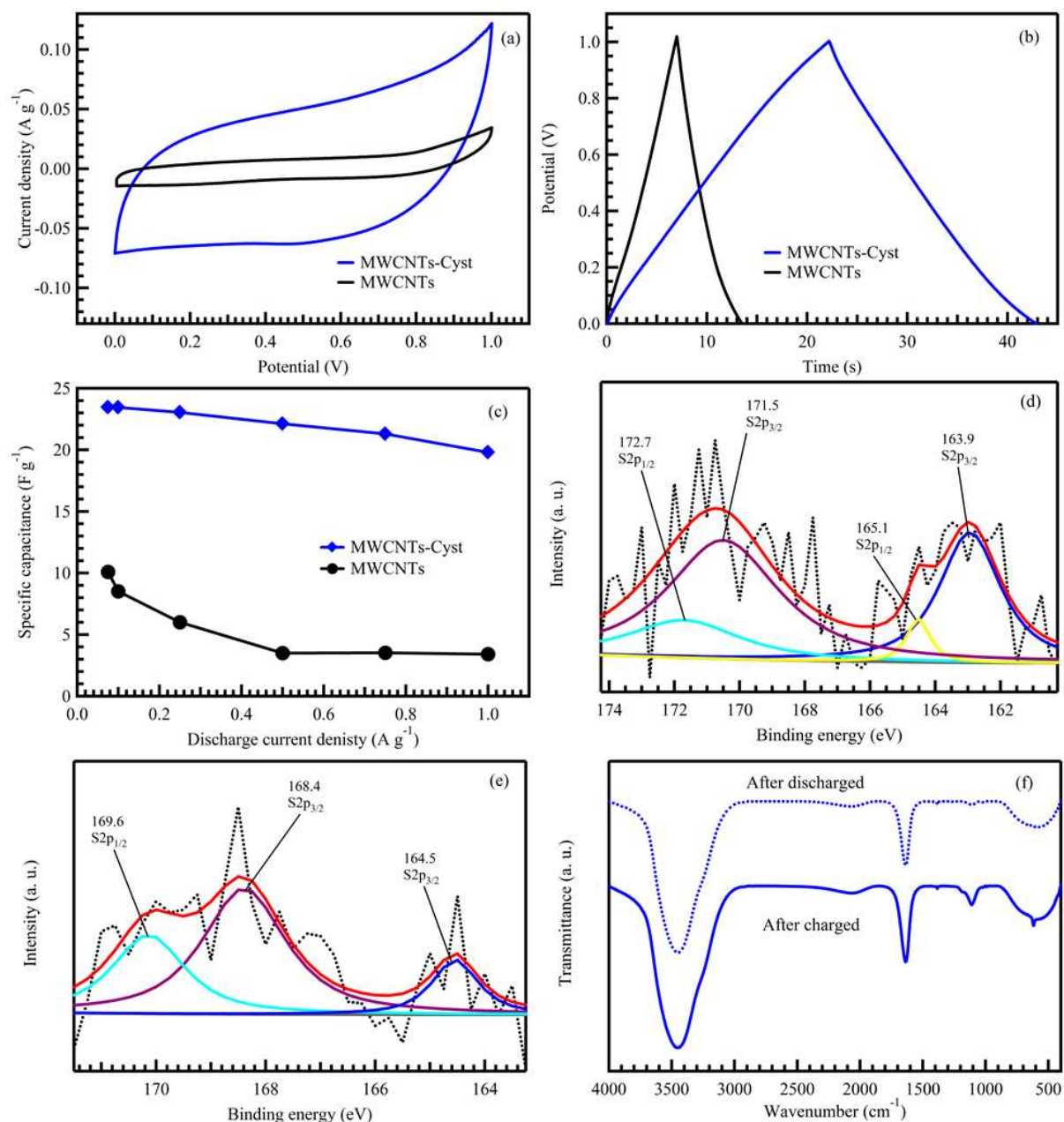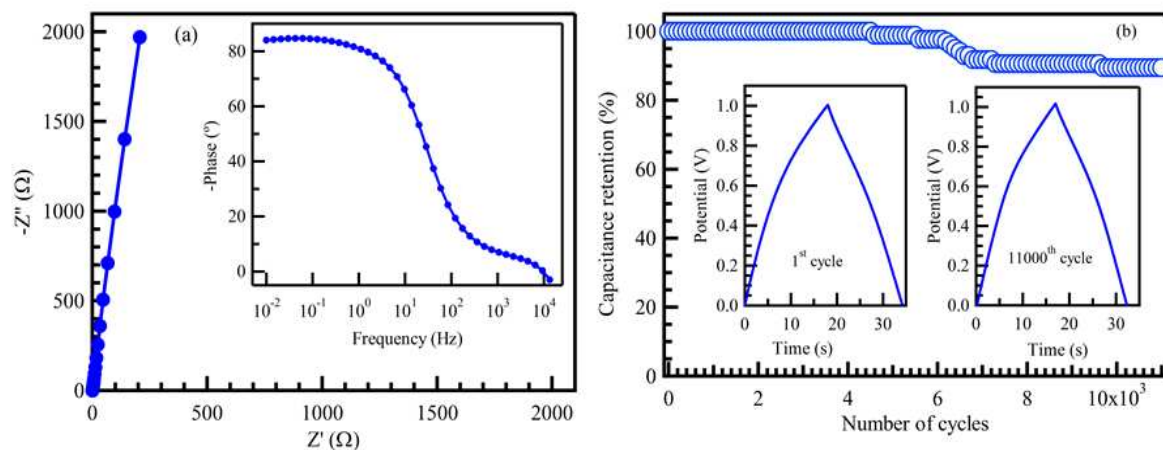
Fig. 2. (a) CV of MWCNTs and MWCNTs-Cyst at 25 mV s^{-1}; (b) CDC of MWCNTs and MWCNTs-Cyst at 0.25 A g^{-1} in 1 M Na$_2$SO$_4$ electrolyte; (c) Specific capacitance as a function of discharge current density; (d) XPS S 2p spectra of MWCNTs-Cyst after charged; (e) XPS S 2p spectra of MWCNTs-Cyst after discharged; (f) FTIR of MWCNTs-Cyst after charged and discharged.

Fig. 3. (a) EIS spectrum for MWCNTs-Cyst (Inset shows the Bode plot for phase angle); (b) Stability test for MWCNTs-Cyst for 11000 cycles (Insets show the CDC of 1st cycle and 11000th cycle).

References

[1] Z. Cao, B.B. Wei, A perspective: carbon nanotube macro-films for energy storage, Energy Environ. Sci., 6 (2013) 3183-3201.

[2] S. Iijima, Helical microtubules of graphitic carbon, Nature, 354 (1991) 56-58.

[3] X. Fan, C. Yu, Z. Ling, J. Yang, J. Qiu, Hydrothermal synthesis of phosphate-functionalized carbon nanotube-containing carbon composites for supercapacitors with highly stable performance, ACS Appl. Mater. Interfaces, 5 (2013) 2104-2110.

[4] W. Shi, J. Chen, Q. Yang, S. Wang, C. Xiong, Novel three-dimensional carbon nanotube–graphene architecture with abundant chambers and its application in lithium–silicon batteries, J. Phys. Chem. C, 120 (2016) 13807–13814.

[5] W. Wang, S. Guo, M. Penchev, I. Ruiz, K.N. Bozhilov, D. Yan, M. Ozkan, C.S. Ozkan, Three dimensional few layer graphene and carbon nanotube foam architectures for high fidelity supercapacitors, Nano Energy, 2 (2013) 294-303.

[6] A.A. Yazdi, L. D'Angelo, N. Omer, G. Windiasti, X. Lu, J. Xu, Carbon nanotube modification of microbial fuel cell electrodes, Biosens. Bioelectron., 85 (2016) 536-552.

[7] M.I. Sajid, U. Jamshaid, T. Jamshaid, N. Zafar, H. Fessi, A. Elaissari, Carbon nanotubes from synthesis to in vivo biomedical applications, Int. J. Pharm., 501 (2016) 278-299.

[8] M. Prodana, M. Duta, D. Ionita, D. Bojin, M.S. Stan, A. Dinischiotu, I. Demetrescu, A new complex ceramic coating with carbon nanotubes, hydroxyapatite and TiO_2 nanotubes on Ti surface for biomedical applications, Ceram. Int., 41 (2015) 6318-6325.

[9] W. Deng, A. Hu, X. Chen, S. Zhang, Q. Tang, Z. Liu, B. Fan, K. Xiao, Sulfur-impregnated 3D hierarchical porous nitrogen-doped aligned carbon nanotubes as high-performance cathode for lithium-sulfur batteries, J. Power Sources, 322 (2016) 138-146.

[10] J. Zhao, J. Ma, X. Nan, B. Tang, Application of non-covalent functionalized carbon nanotubes for the counter electrode of dye-sensitized solar cells, Org. Electron., 30 (2016) 52-59.

[11] C.-Y. Ma, S.-C. Huang, P.-H. Chou, W. Den, C.-H. Hou, Application of a multiwalled carbon nanotube-chitosan composite as an electrode in the electrosorption process for water purification, Chemosphere, 146 (2016) 113-120.

[12] C. Zhang, M. Li, X. Xu, N. Liu, Effects of carbon nanotubes on atrazine biodegradation by Arthrobacter sp., J. Hazard. Mater., 287 (2015) 1-6.

[13] C. Fu, H. Zhou, R. Liu, Z. Huang, J. Chen, Y. Kuang, Supercapacitor based on electropolymerized polythiophene and multi-walled carbon nanotubes composites, Mater. Chem. Phys., 132 (2012) 596-600.

[14] S. Hussain, R. Amade, E. Bertran, Study of CNTs structural evolution during water assisted growth and transfer methodology for electrochemical applications, Mater. Chem. Phys., 148 (2014) 914-922.

[15] K. Naoi, T. Kurita, M. Abe, T. Furuhashi, Y. Abe, K. Okazaki, J. Miyamoto, E. Iwama, S. Aoyagi, W. Naoi, Ultrafast nanocrystalline-TiO_2(B)/carbon nanotube hyperdispersion prepared via combined ultracentrifugation and hydrothermal treatments for hybrid supercapacitors, Adv. Mater., 28 (2016) 6751-6757.

[16] J. Zhou, J. Chen, S. Han, H. Zhao, J. Bai, Z. Yang, X. Mu, Y. Liu, D. Bian, G. Sun, Constructing optimized three-dimensional electrochemical interface in carbon nanofiber/carbon nanotube hierarchical composites for high-energy-density supercapacitors, Carbon, 111 (2017) 502-512.

[17] J. Wang, W. Dou, X. Zhang, W. Han, X. Mu, Y. Zhang, X. Zhao, Y. Chen, Z. Yang, Q. Su, E. Xie, W. Lan, X. Wang, Embedded Ag quantum dots into interconnected Co_3O_4 nanosheets grown on 3D graphene networks for high stable and flexible supercapacitors, Electrochim. Acta, 224 (2017) 260-268.

[18] C. Niu, E.K. Sichel, R. Hoch, D. Moy, H. Tennent, High power electrochemical capacitors based on carbon nanotube electrodes, Appl. Phys. Lett., 70 (1997) 1480-1482.

[19] E. Frackowiak, F. Beguin, Electrochemical storage of energy in carbon nanotubes and nanostructured carbons, Carbon, 40 (2002) 1775-1787.

[20] C. Li, D. Wang, T. Liang, X. Wang, L. Ji, A study of activated carbon nanotubes as double-layer capacitors electrode materials, Mater. Lett., 58 (2004) 3774-3777.

[21] H. Liu, H. Song, X. Chen, S. Zhang, J. Zhou, Z. Ma, Effects of nitrogen- and oxygen-containing functional groups of activated carbon nanotubes on the electrochemical performance in supercapacitors, J. Power Sources, 285 (2015) 303-309.

[22] H. Sadegh, K. Zare, B. Maazinejad, R. Shahryari-ghoshekandi, I. Tyagi, S. Agarwal, V.K. Gupta, Synthesis of MWCNT-COOH-Cysteamine composite and its application for dye removal, J. Mol. Liq., 215 (2016) 221-228.

[23] K.Y.T. Lee, H.H. Shi, K. Lian, H.E. Naguib, Flexible multiwalled carbon nanotubes/conductive polymer composite electrode for supercapacitor applications, Smart Mater. Struct., 24 (2015) 115008–115015.

[24] W.S.V. Lee, M. Leng, M. Li, X.L. Huang, J.M. Xue, Sulphur-functionalized graphene towards high performance supercapacitor, Nano Energy, 12 (2015) 250-257.

[25] L. Yang, S. Cheng, Y. Ding, X. Zhu, Z.L. Wang, M. Liu, Hierarchical network architectures of carbon fiber paper supported cobalt oxide nanonet for high-capacity pseudocapacitors, Nano Lett., 12 (2011) 321-325.

[26] M.S. Kishore, P. Srimathi, S. Kumar, S. Addepalli, S. Swaminathan, V. Tilak, R. Colborn, Combustion synthesis of graphene and ultracapacitor performance, Bull. Mater. Sci., 36 (2013) 667–672.

[27] S.H. Aboutalebi, M. Salari, K. Konstantinov, D. Wexler, H.K. Liu, S.X. Dou, Comparison of GO, GO–MWCNTs composite, Energy Environ. Sci., 4 (2011) 1855–1865.

[28] E.Y.L. Teo, H.N. Lim, R. Jose, K.F. Chong, Aminopyrene functionalized reduced graphene oxide as a supercapacitor electrode, RSC Adv., 5 (2015) 38111-38116.

[29] S.K. Park, Q. Mahmood, H.S. Park, Surface functional groups of carbon nanotubes to manipulate capacitive behaviors, Nanoscale, 5 (2013) 12304–12309.

Highlights

- 4-times capacitance enhancement by functionalizing MWCNTs with cysteamine groups
- Oxidation of thiol into sulfinic acid in cysteamine during functionalization
- Redox reaction of sulfinic acid and sulfenic acid during charge discharge
- High cycling stability (90%) of MWCNTs-Cyst